Electronic Supplementary Information (ESI)

Photo-triggered transformation from vesicles to branched nanotubes fabricated by a cholesterol-appended cyanostilbene

Pengyao Xing,[a, c] Hongzhong Chen,[a] Linyin Bai[a] and Yanli Zhao[*a, b]

[a]*Division of Chemistry and Biological Chemistry, School of Physical and Mathematical Sciences, Nanyang Technological University, 21 Nanyang Link, Singapore 637371, Singapore. E-mail: zhaoyanli@ntu.edu.sg*
[b]*School of Materials Science and Engineering, Nanyang Technological University, Singapore 639798, Singapore*
[c]*School of Chemistry and Chemical Engineering and Key Laboratory of Colloid and Interface Chemistry of Ministry of Education, Shandong University, Jinan 250100, PR China*

1. Experimental section

Materials

All chemicals were purchased from Sigma-Aldrich and used without further purification. Before use, acetone was re-distilled under reflux with potassium carboxylate. (Z)-3-(4-(Dimethylamino) phenyl)-2-(4-hydroxyphenyl)acrylonitrile (compound 1) was synthesized according to our previous report[S1].

Characterizations

^{1}H NMR spectra were measured on a Bruker-AC 300 spectrometer. ^{13}C NMR spectrum was measured on a Bruker BBFO-400 spectrometer. The electronic spray ionization (ESI) mass spectra were recorded on a ThermoFinnigan LCQ quadrupole ion trap mass spectrometer. High-resolution mass spectrometry (HR-MS) was performed on a Waters Q-tof Premier MS spectrometer. Absorption spectra were recorded on a Shimadzu UV-3600 spectrophotometer. The fluorescence emission spectra were recorded on a Shimadzu RF-5301pc fluorescence spectrophotometer. The photoirradiation was carried on an ENF-260C/FBE UV lamp (4 W) with the irradiation wavelength of 254 nm in a 2 mm quartz cell. TEM images were collected on a JEM-1400 (JEOL). SEM images were collected from a SEM of field-emission JSM-6700F (JEOL). DLS size distributions were measured on a Nanobrook 90Plus particle size analyzer.

Synthesis of CSC

A solution of cholesteryl chloroformate (0.50 g, 1.1 mmol) in anhydrous acetone (20 mL) was added dropwise into a mixed solution of compound 1 (0.27 g, 1.0 mmol) and triethylamine (0.1 mL) in anhydrous acetone (20 mL) at 0 ^{o}C. The mixture was stirred at room temperature for 1h. Then, the mixture was filtered to remove the byproduct. The filtrate was concentrated under reduced pressure and the residue was recrystallized three times (ethyl acetate/hexane, 1:10, v/v) to obtain the pure yellow compound CSC (500 mg, 74%). ^{1}H NMR (300 MHz, $CDCl_3$, 298 K). δ = 7.83 (d, 2H), 7.63 (d, 2H), 7.36 (s, 1H), 7.22 (d, 2H), 6.73 (d, 2H), 5.43 (s, 1H), 4.57 (m, 1H), 3.06 (s, 6H), .50 (d, 2H), 2.0-0.85 (m, 41H). ^{13}C NMR (100 MHz, $CDCl_3$, 298 K) δ = 152.66, 151.71, 151.45, 144.61, 142.65, 138.98, 133.22, 131.63, 131.19, 130.02, 126.39, 123.13, 121.27, 119.21, 111.16, 106.12, 103.18, 78.98, 56.53, 56.00, 49.03, 42.15, 40.02, 39.98, 39.66, 39.40, 37.86, 36.77, 36.49, 36.11, 35.60, 31.74, 31.85, 30.03, 28.17, 27.90, 27.57, 24.16, 23.70, 22.73, 22.48, 20.85, 19.19, 18.59, 11.59. HRMS (TOF) m/z $[M+H]^+$, calcd for $C_{45}H_{61}N_2O_3$, 677.4682; found, 677.4666.

Preparation of hydrogen peroxide (H_2O_2)

Concentrated H_2O_2 (30 wt%) was diluted in deionized (DI) water to 10 mM and stirred for 10 min before used.

Preparation of hydroxyl radical (·OH)

H_2O_2 was diluted in DI water and $FeSO_4·7H_2O$ was dissolved in DI water, respectively. Then the $FeSO_4·7H_2O$ solution (finally 1 mM) was dropped into H_2O_2 solution (finally 10 mM).

Preparation of singlet oxygen ($^1O_2$)

NaClO solution was dropped into diluted H_2O_2 solution (1 mM) to make a 10 mM solution, which was then stirred at room temperature for 30 min.

Preparation of hypochlorite (ClO^-)

Concentrated sodium hypochlorite (3 M) was diluted in DI water to 10 mM and stirred for 10 min before used.

2. Self-assembly behavior of CSC

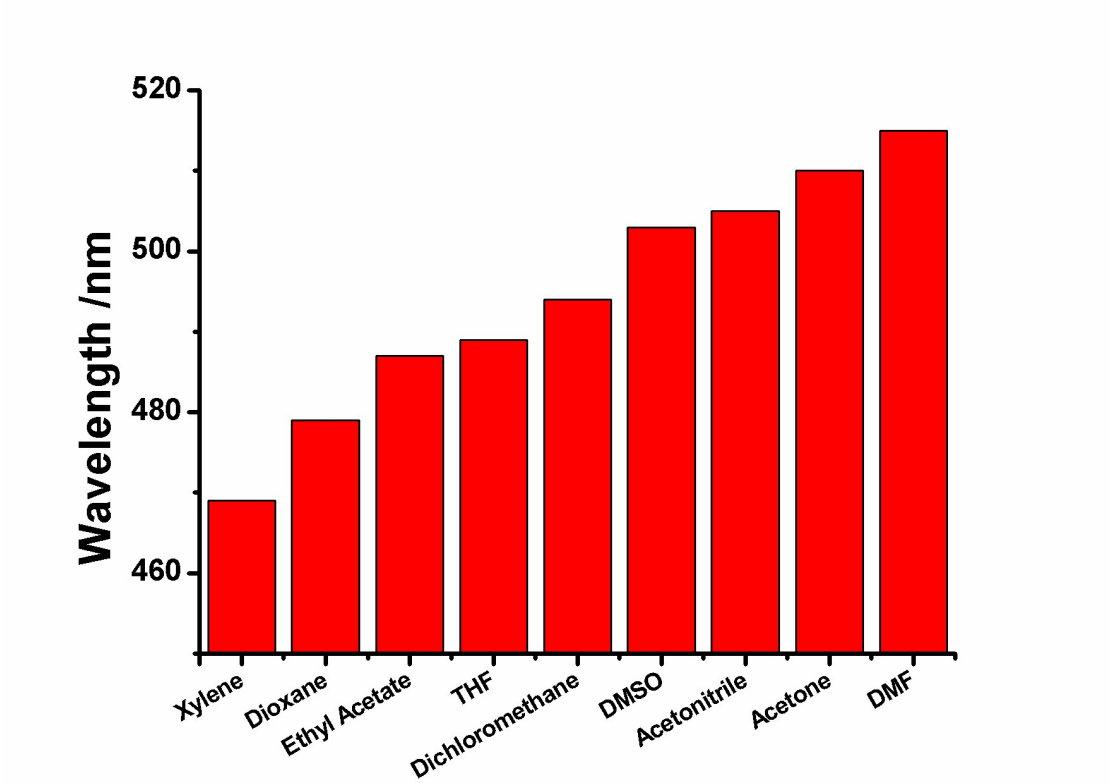

Figure S1. The maximum emission wavelengths of CSC in different solvents.

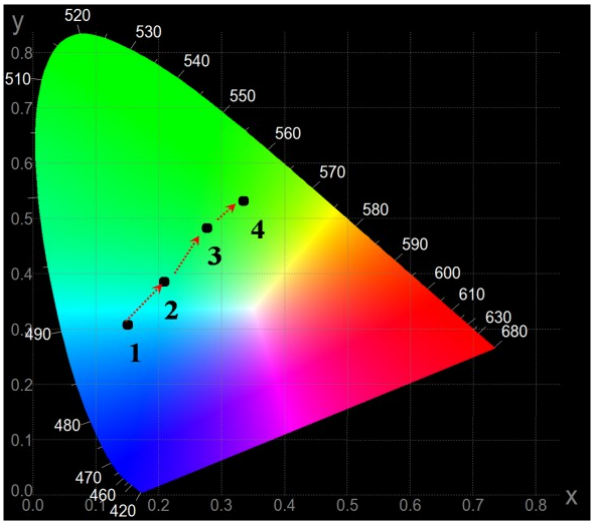

Figure S2. CIE 1931 chromaticity diagram (c). The black dots indicate the luminescent color coordinates of the states 1 (0.15, 0.31), 2 (0.21, 0.38), 3 (0.28, 0.49) and 4 (0.32, 0.54), corresponding to samples in 0/10, 8/2, 9/1 and 9.5/0.5 H_2O/THF solution (v/v).

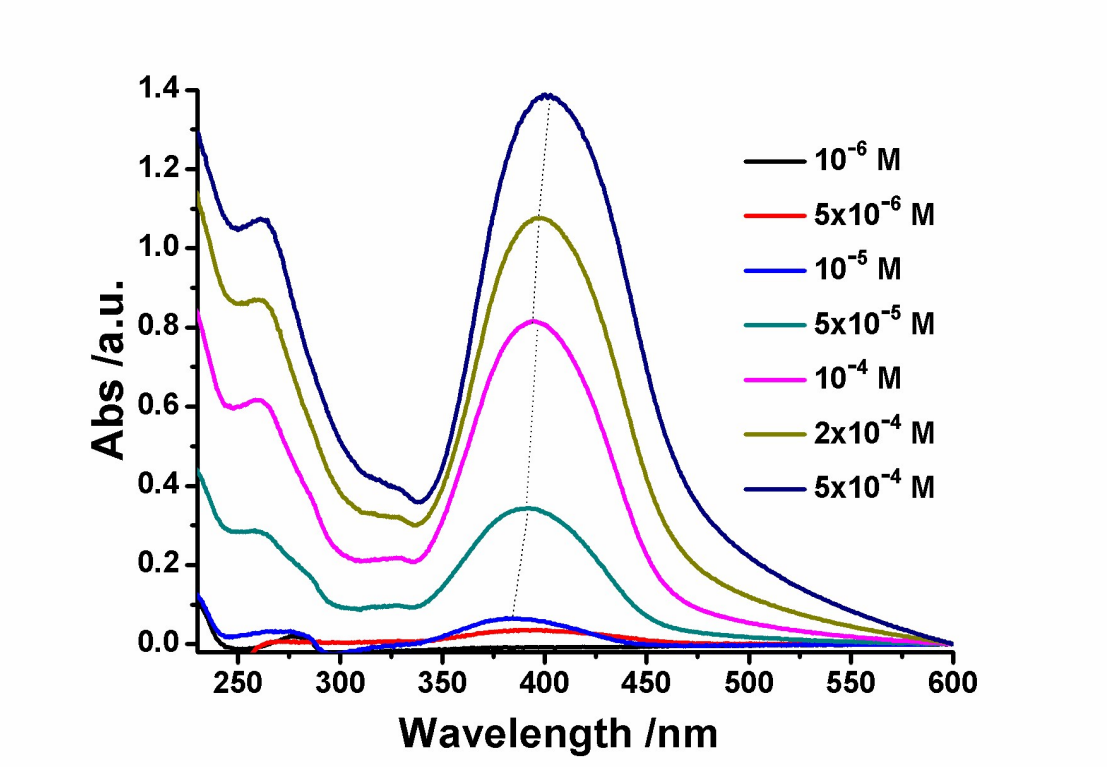

Figure S3. Concentration dependent absorption spectra of CSC in H_2O/THF mixture (9/1, v/v).

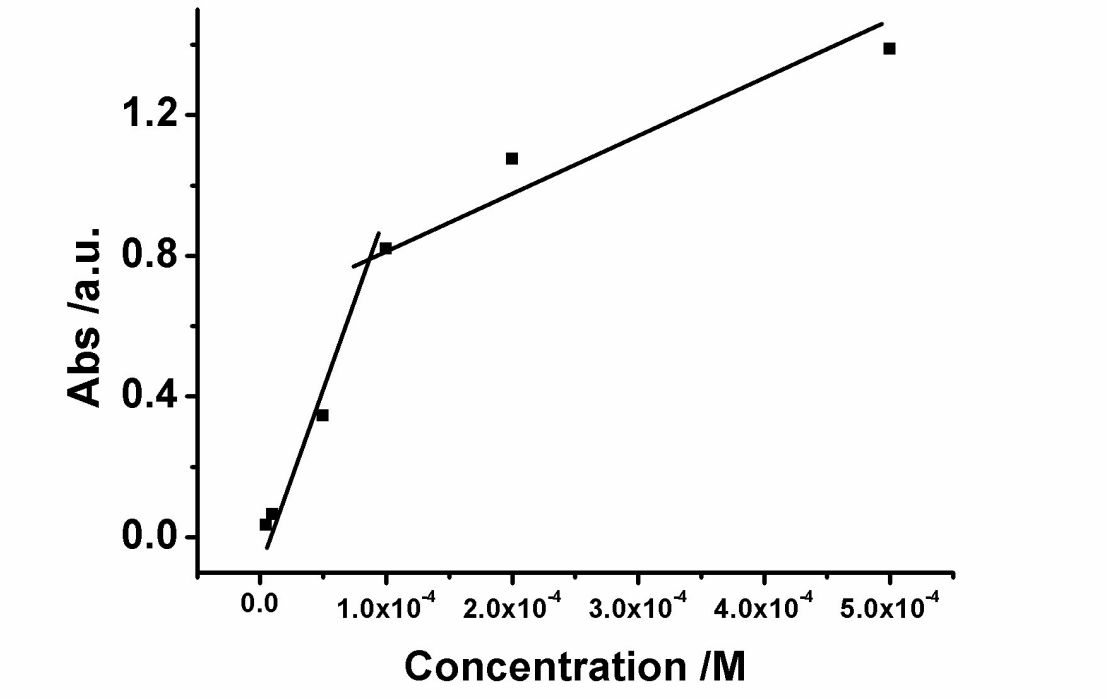

Figure S4. Maximum absorption changes as a function of CSC concentrations in H_2O/THF mixture (9/1, v/v).

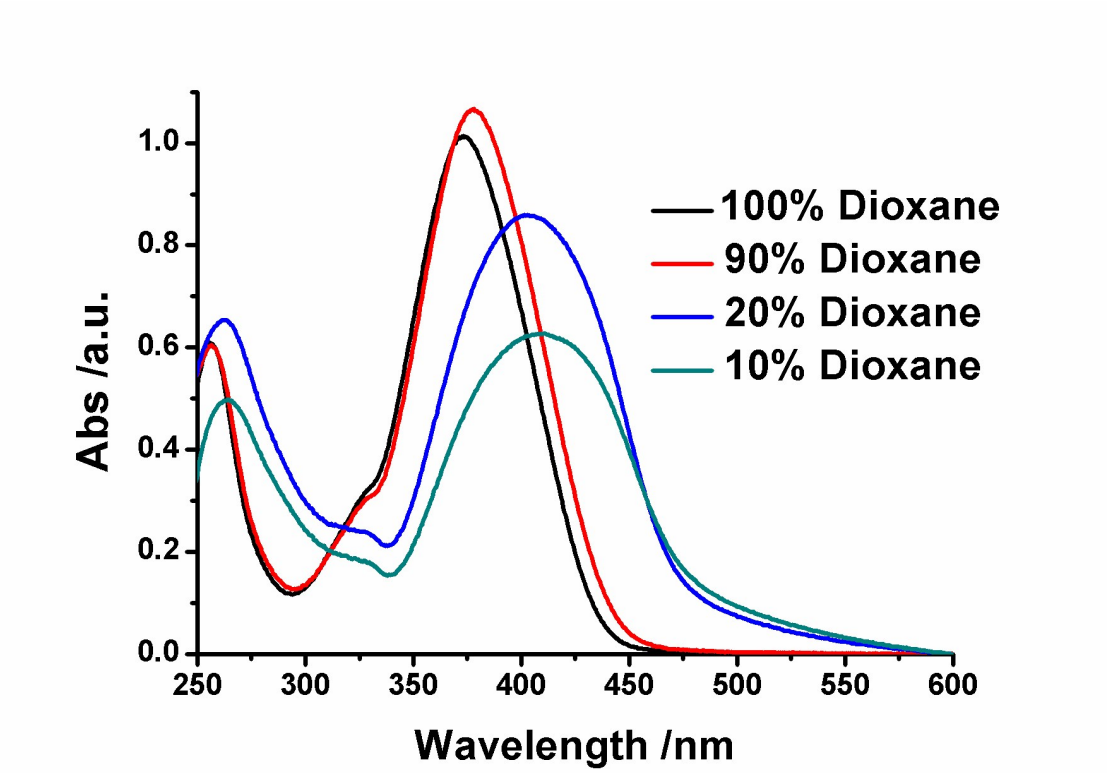

Figure S5. Absorption spectra of CSC (10^{-4} M) in different solvents of dioxane and water.

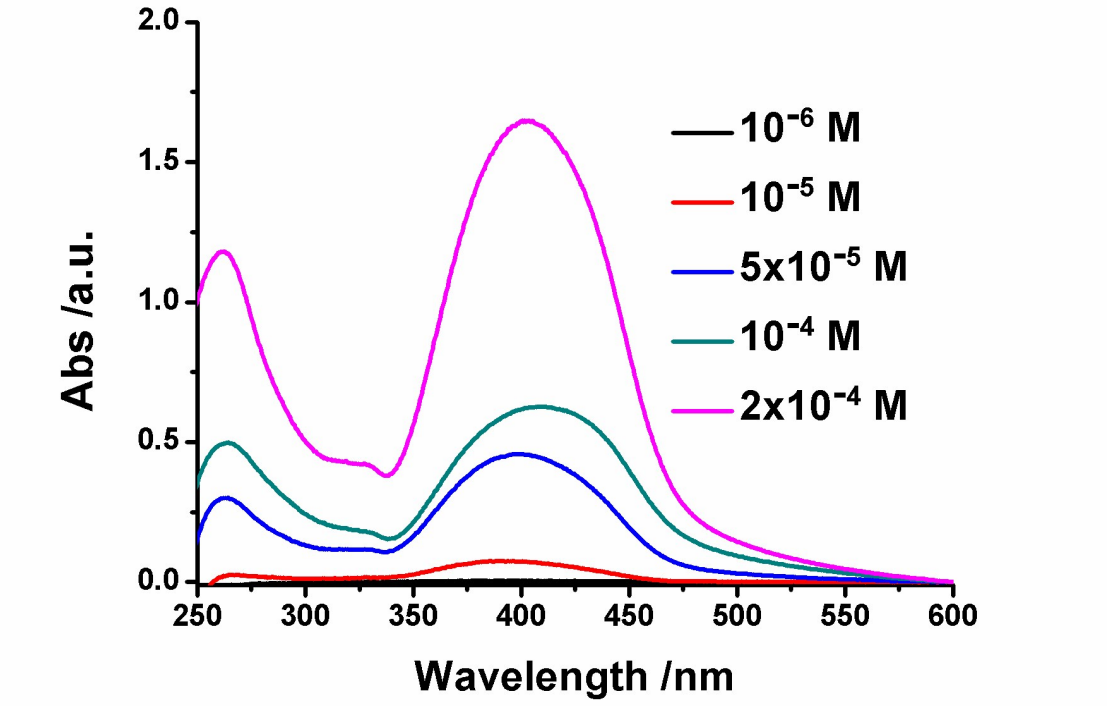

Figure S6. Concentration dependent absorption spectra of CSC in mixed solvents of H_2O/dioxane (9/1, v/v).

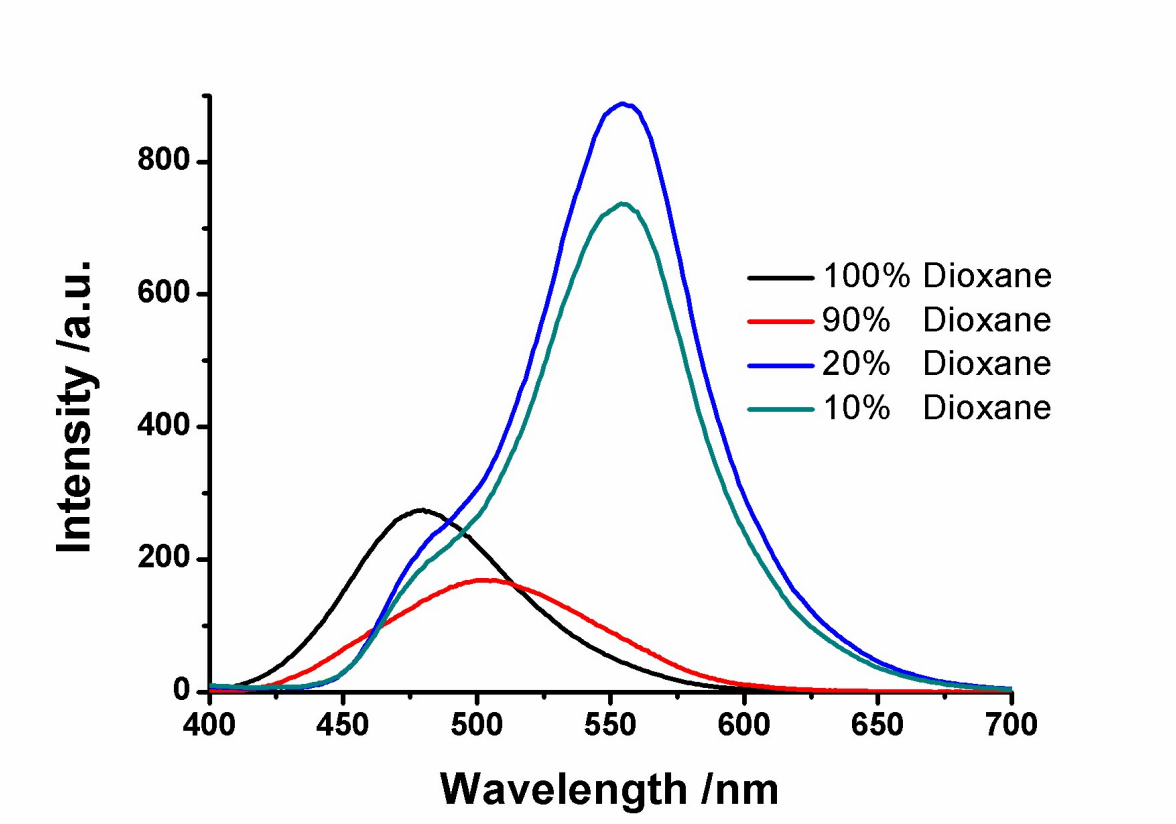

Figure S7. Emission spectra of CSC (10^{-4} M) in different solvents of water and dioxane.

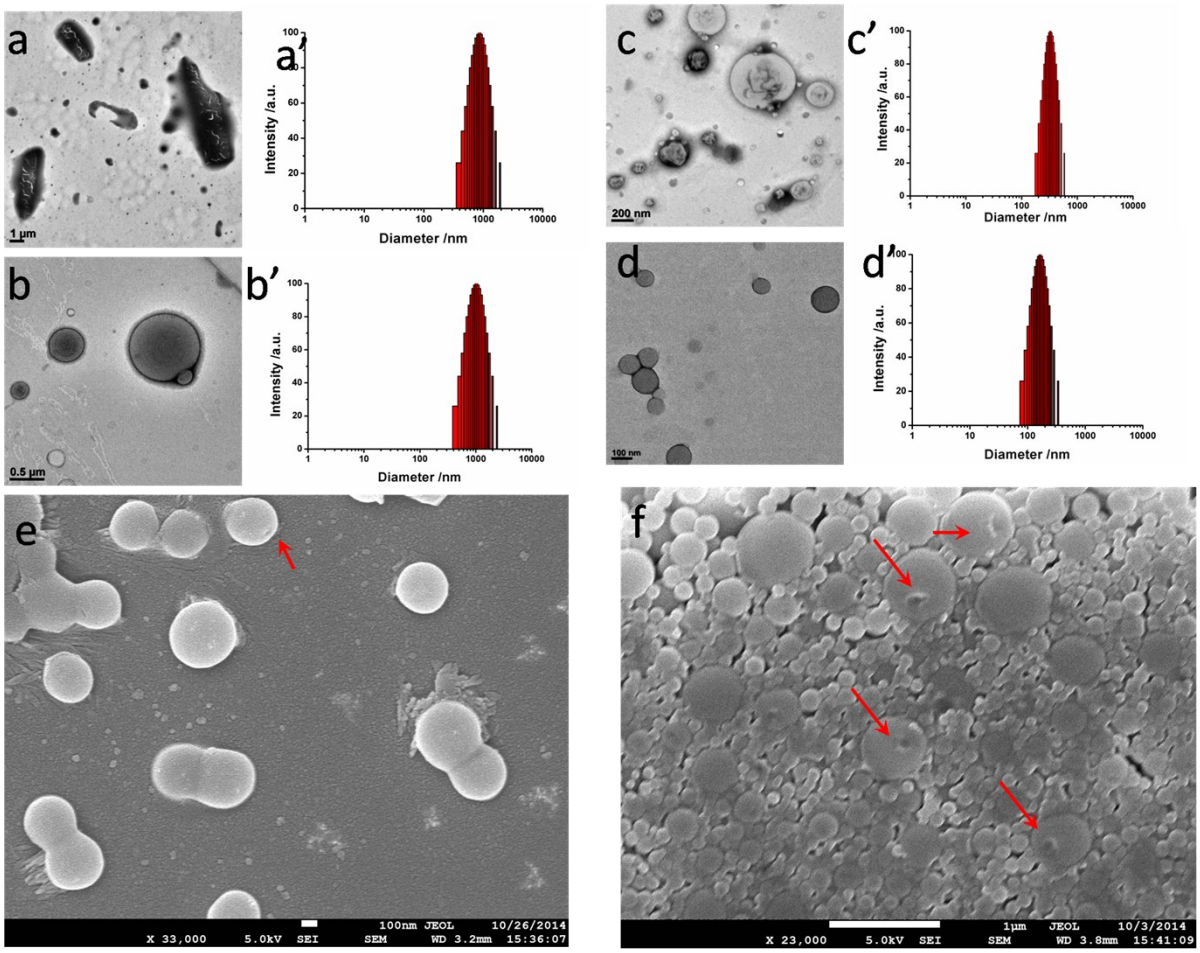

Figure S8. Negatively stained TEM images and DLS size distributions of CSC (10^{-4} M) based vesicles in H_2O/THF mixture: a,a' (5/5, v/v), b,b' (6/4, v/v), c,c' (7/3, v/v), and d,d' (8/2, v/v). SEM images of vesicles (e: H_2O/dioxane, 8/2, v/v; f: H_2O/THF, 7/3, v/v)

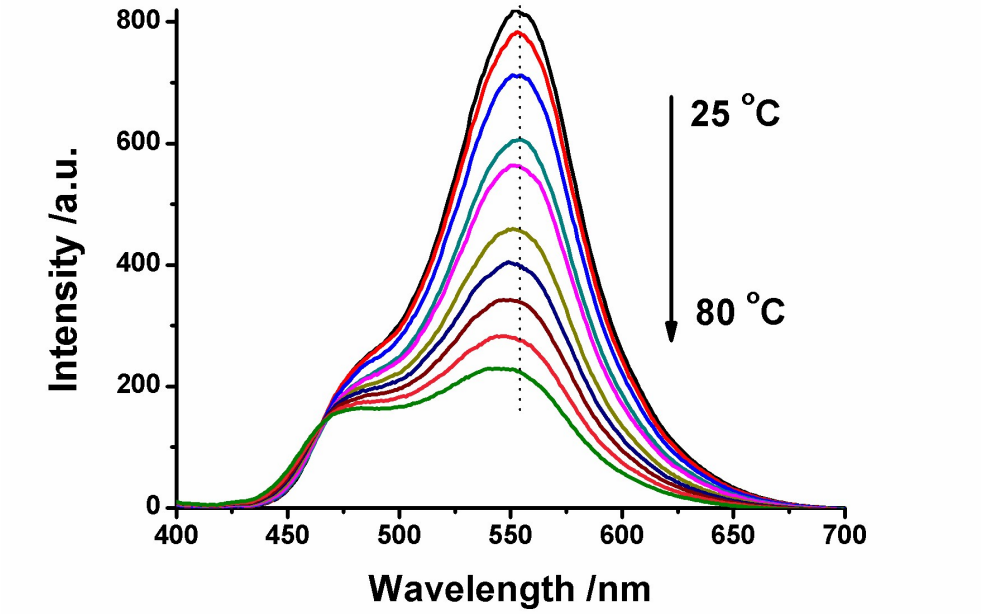

Figure S9. Temperature-dependent emission spectra of CSC in H_2O/dixane mixture (9/1, v/v).

3. UV light responsiveness

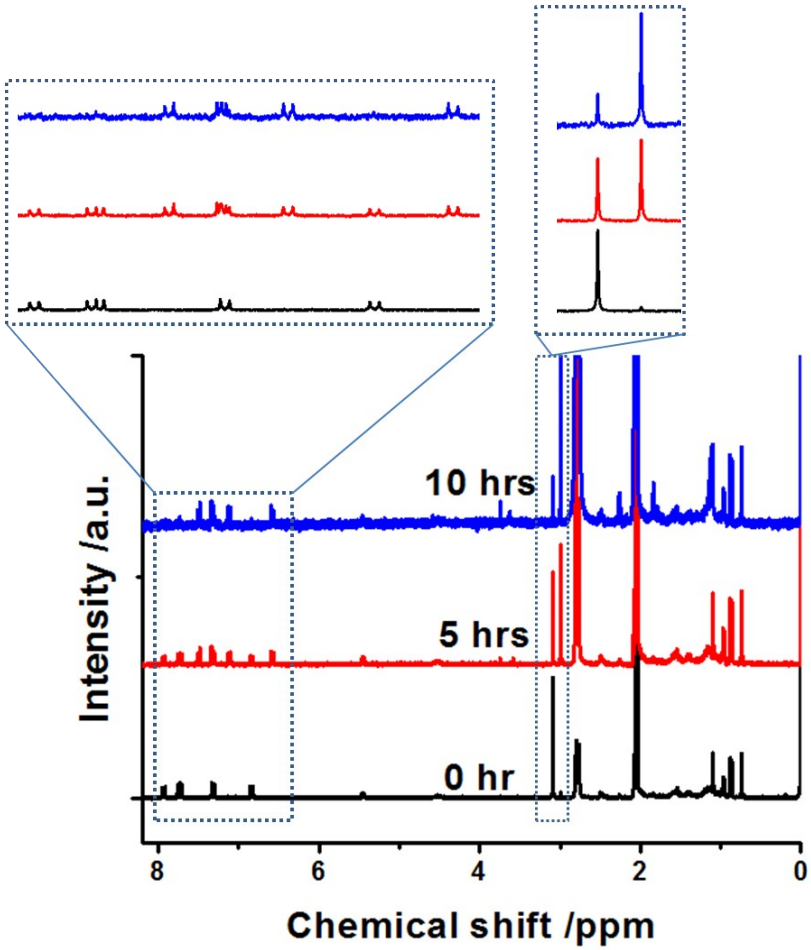

Figure S10. ^{1}H NMR spectral comparison of CSC in acetone-D_6 under different UV irradiation times.

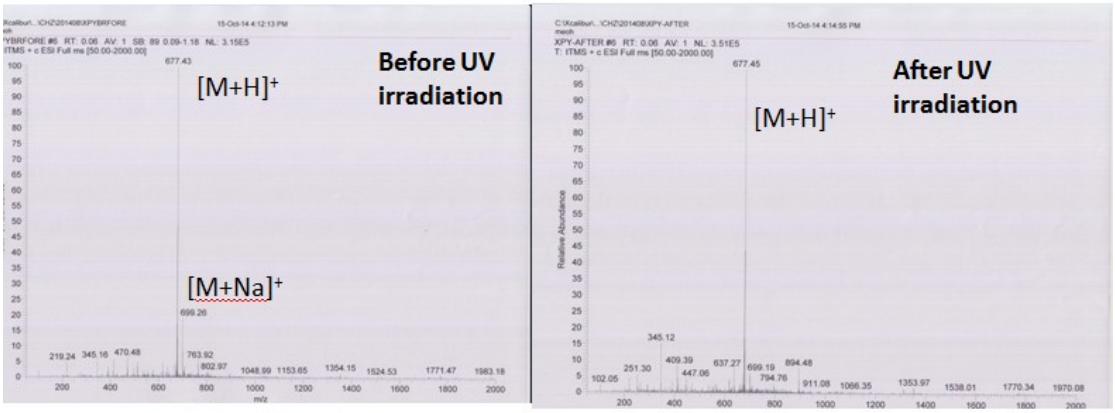

Figure S11. Mass spectral comparison of CSC before and after sufficient UV light irradiation.

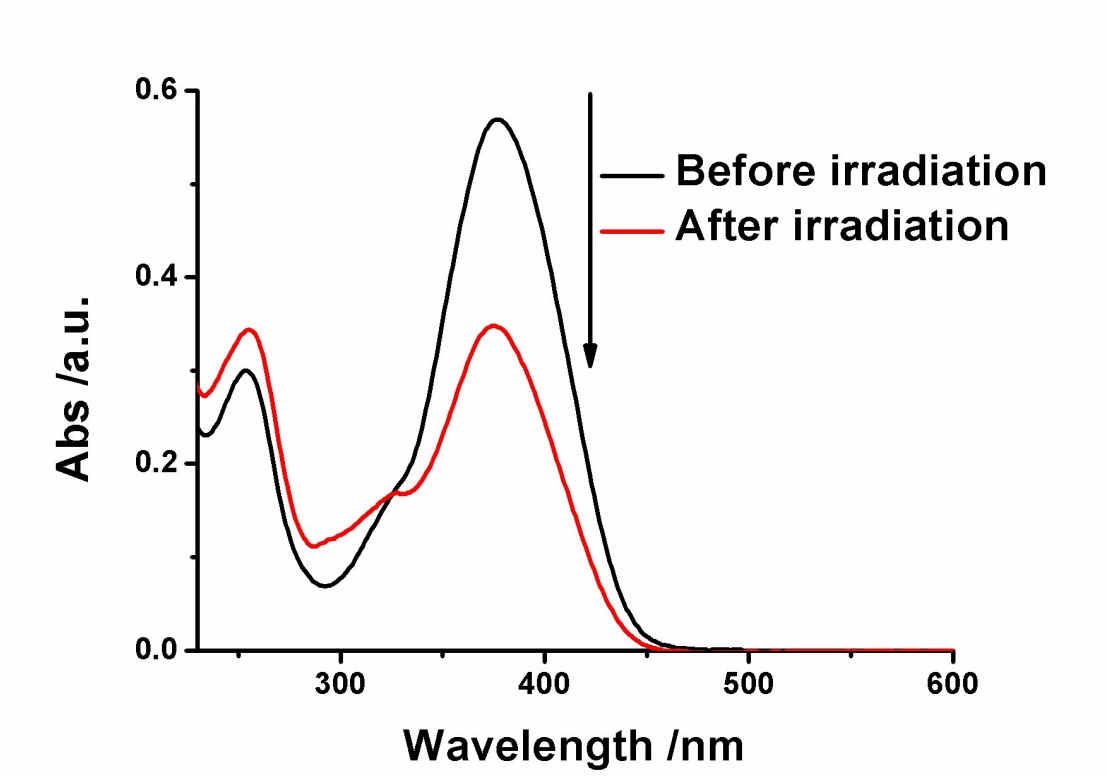

Figure S12. Absorption spectra of CSC in pure THF before and after UV light irradiation.

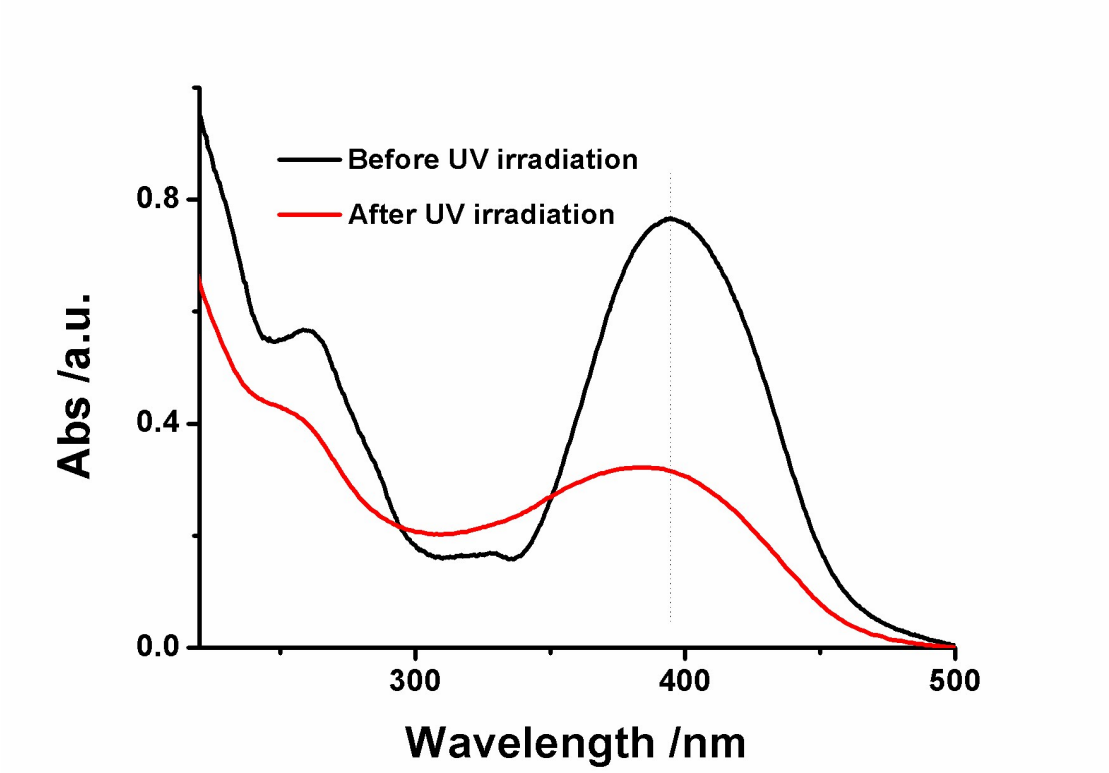

Figure S13. Absorption spectra of CSC (10^{-4} M) in H_2O/THF mixture (9/1, v/v) before and after UV light irradiation.

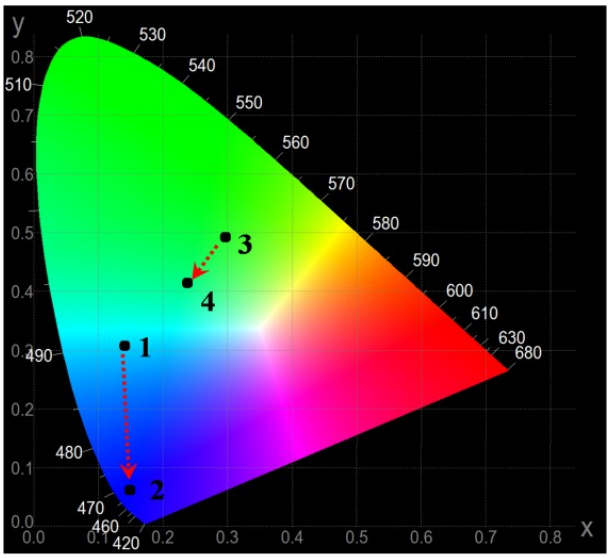

Figure S14. CIE 1931 chromaticity diagram. The black dots stand for the luminescent color coordinates of the states 1 (0.15, 0.31), 2 (0.15, 0.07), 3 (0.28, 0.49), and 4 (0.24, 0.42), representing the samples in 100 vol% THF (1) with and (2) without UV light irradiation (irradiation time: 8h), and in 10 vol% THF (3) with and (4) without UV light irradiation (irradiation time: 8h).

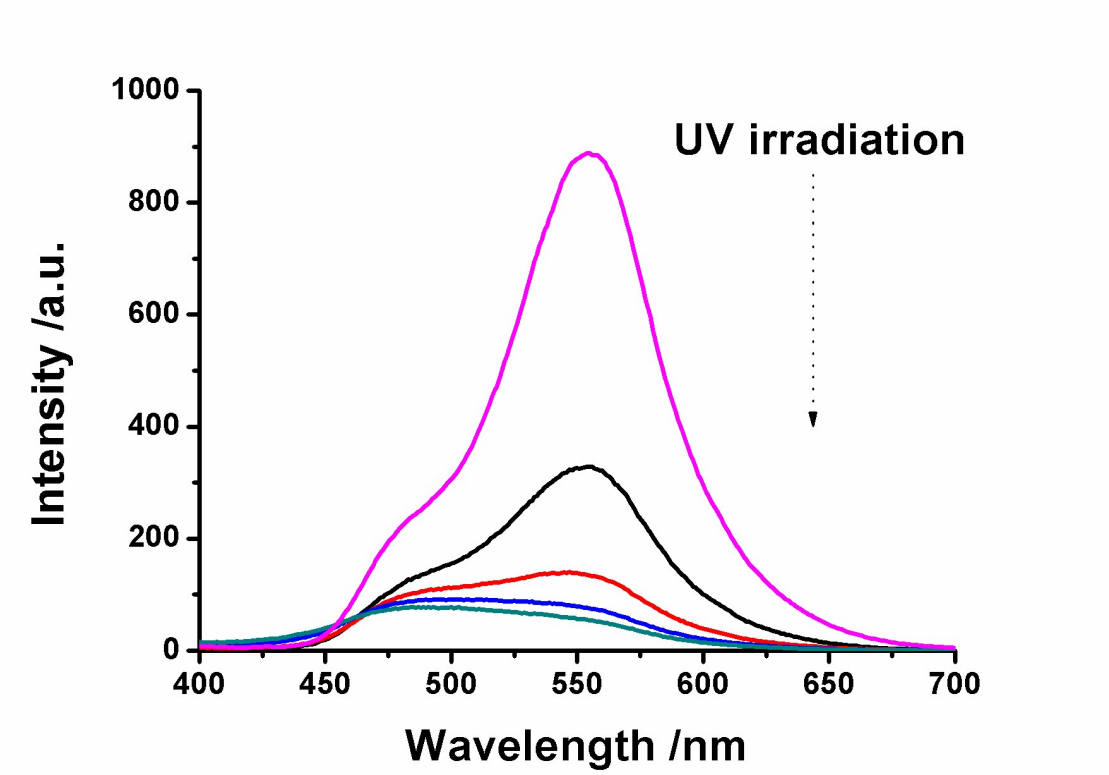

Figure S15. Emission spectral changes of CSC (10^{-4} M) in H_2O/dioxane mixture (9/1, v/v) upon UV light irradiation with irradiation time of 0h, 2h, 4h, 6h, and 8h.

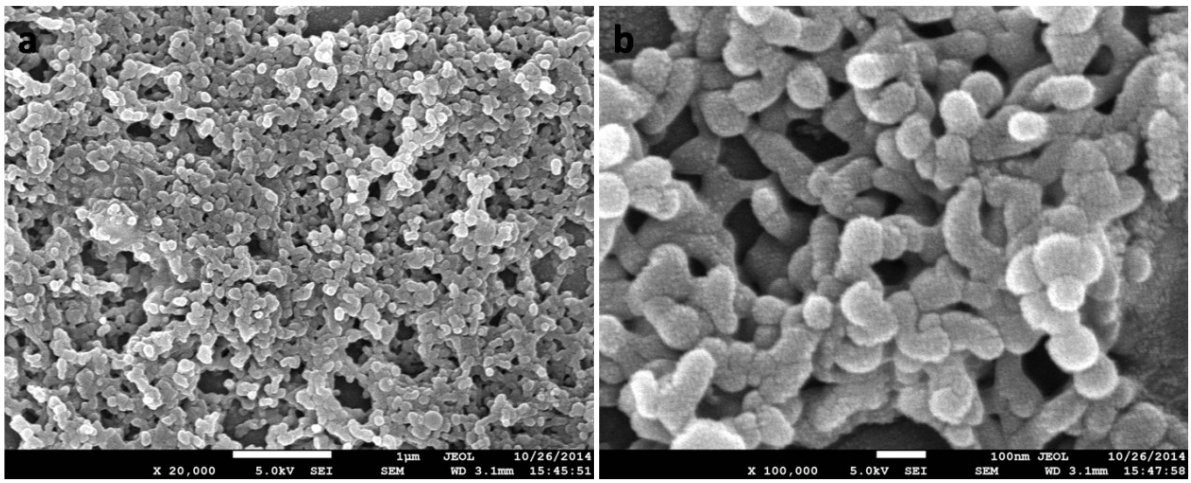

Figure S16. SEM images of CSC (10^{-4} M) in H_2O/THF (9/1, v/v) after UV light irradiation.

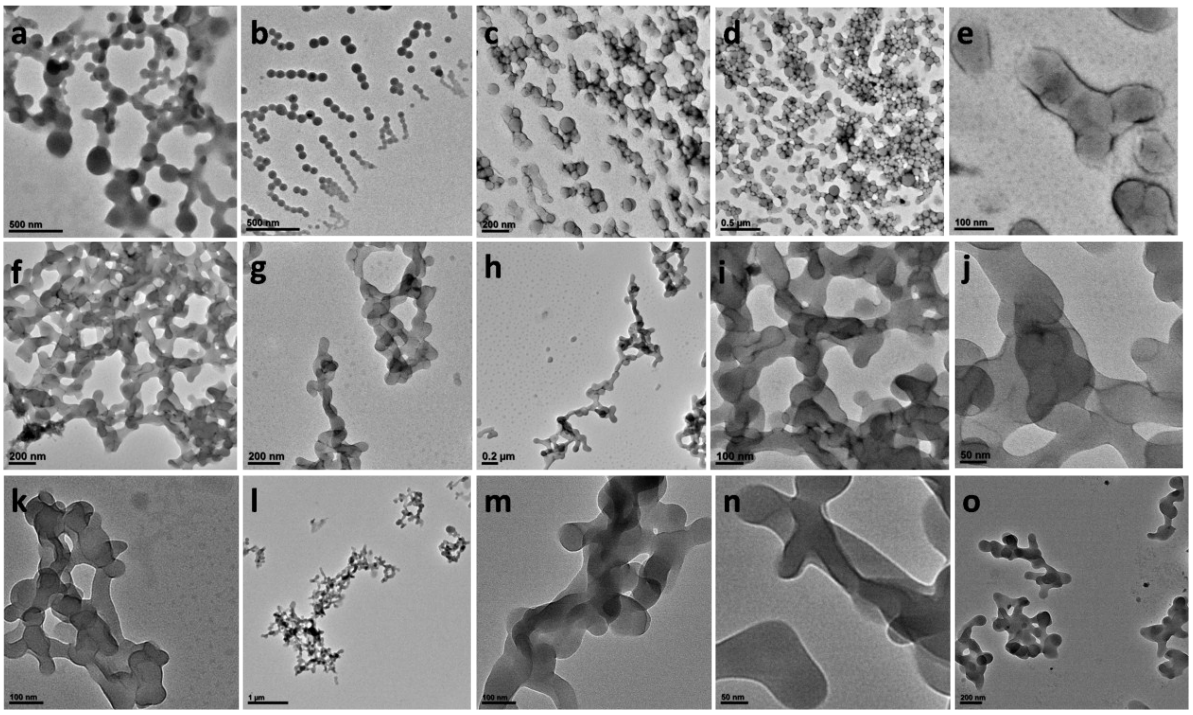

Figure S17. TEM images of CSC (10^{-4} M) in mixture solvent upon UV light irradiation: a-e (H_2O/THF, 9/1, v/v, short time irradiation), f-j (H_2O/THF, 9/1, v/v, long time irradiation), k-n (H_2O/dioxane, 8/2, v/v, short time irradiation), o (H_2O/dioxane, 8/2, v/v, long time irradiation).

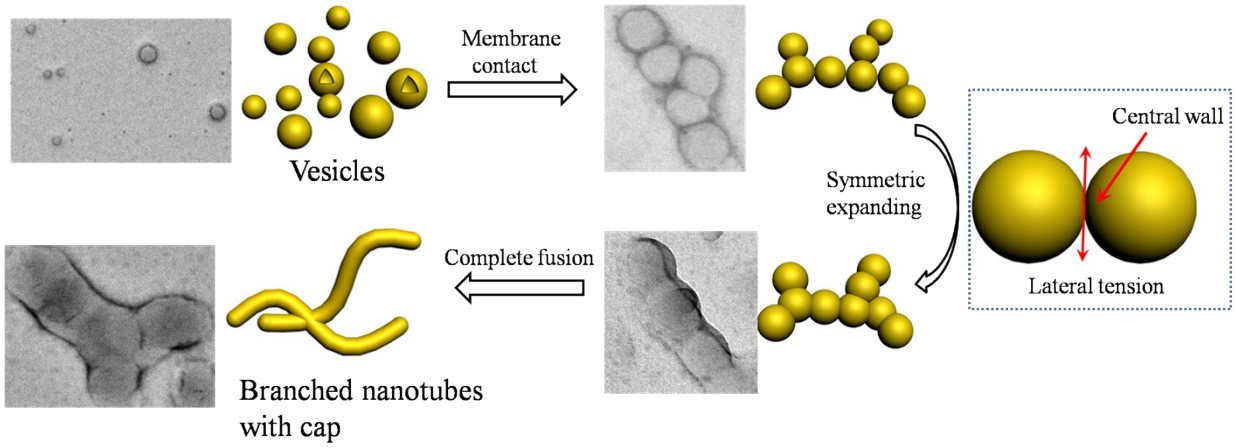

Figure S18. Schematic representation of vesicle to branched/capped nanotube transition process.

Discussions regarding the vesicle fusion process

The original perturbation was caused by the isomerization of CSC that deforms the well-defined π-π stacking interaction, as evidenced by ^{1}H NMR, UV and emission spectra. Similar to previously reported results regarding the vesicle fusion,[S2] we also investigated the perturbation by obtaining the TEM images of surface-contacted vesicles as well as by observing the fusion process step by step. As displayed in Fig. 2g,h, after UV irradiation under short time, vesicles made the surface contact first, followed by the formation of dimeric, trimeric, oligomeric and necklace-like vesicles (arrows in Fig. 2h, S17a-e and S18). The fusion process and its mechanism are slightly different from the fusion process of some giant polymersomes induced by sonication or UV irradiation. The perturbation from isomerization could be understood as follows. It is well know that vesicles in solution may undergo reversible surface contact randomly ascribed to the Brownian movement of colloidal particles[S3], but only few vesicles can fuse into dimeric or larger vesicles in the present case. This is because that the spherical bilayer membrane topology is relatively stable due to appropriate solvophilic and solvaphobic volume ratio of *trans*-CSC. After the isomerization casued by UV irradiation, however, spherical topology became metastable due to the variation of molecular packing parameter ($p = v/la$).[S4] *Cis*-cyanostilbene has more molecular rigidity than *trans*-form, which may decrease the solvophilic area a of CSC, leading to the increase of p value. The increase of p value would favor the formation of more planar bilayer packing mode (nanotubes) rather than spherical bilayer packing mode (vesicles).[S5] Directed by the Brownian movement, occasional surface contact of vesicles may become irreversible, followed by the fusion process.

Schematic representation of detailed fusion process is shown in Fig. S18. The process can be explained as follows based on the TEM observations. 1) Surface contact of vesicles. Brownian movement allows the collision and encounter of vesicles in solution. Due to the decreased solvophilic volume of CSC after photoisomerization, *cis*-CSC has higher intermolecular affinity, which hinders the departure of the attached vesicles and improves their linkage in turn. 2) Central wall formation. After membrane contact, different vesicles would implant into each other to generate a bilayer membrane between two fused vesicles. 3) Expanding contact areas. Induced by the lateral tension of contact areas between vesicles, the central wall between dimeric vesicles diminishes gradually. Notably, the lateral tension may be derived from the molecular rearrangement of *cis*-CSC from *J*-type stacking into face-to-face *H*-type one. After that, the fusion process would be completed.

Instead of giant vesicles, the vesicles transform into nanotubes by fusion. As abovementioned, the change of molecular packing parameter favors one-dimensional nanotube formation due to face-to-face *H*-type π-π stacking array of *cis*-cyanostilbene. Another reason is that giant vesicles own lower curvature values, which may not be favorable in high polarity solvent environments (with up to 80 vol% or more water).

4. Hydrogen peroxide detection

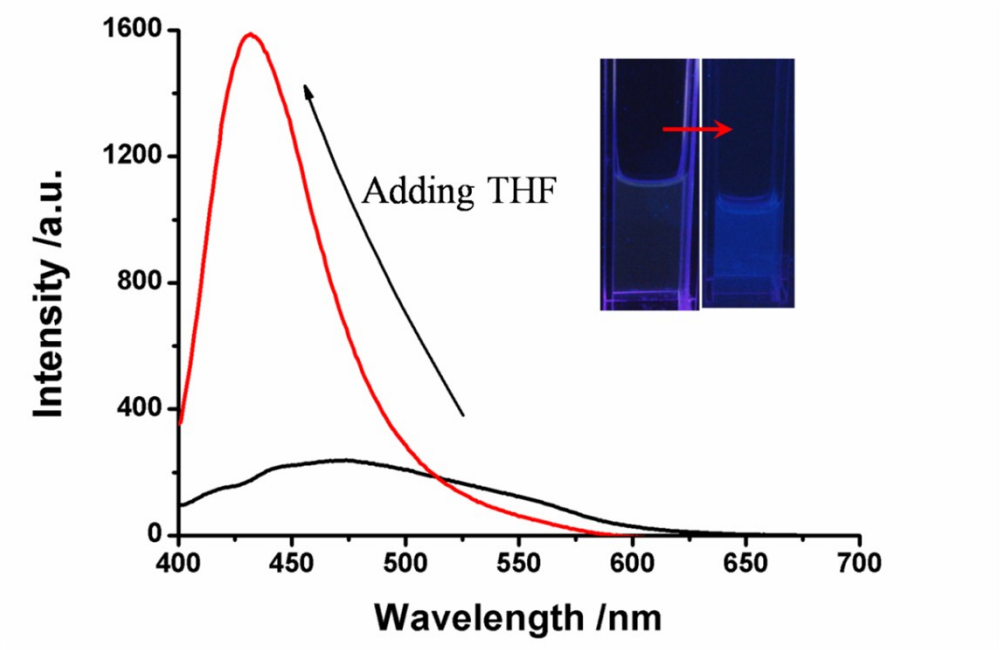

Figure S19. Fluorescence changes upon the addition of H_2O/THF (5/5, v/v) into UV light treated sample (10^{-4}) in H_2O/THF (9/1, v/v). Inset: solution color changes under UV lamp (365 nm).

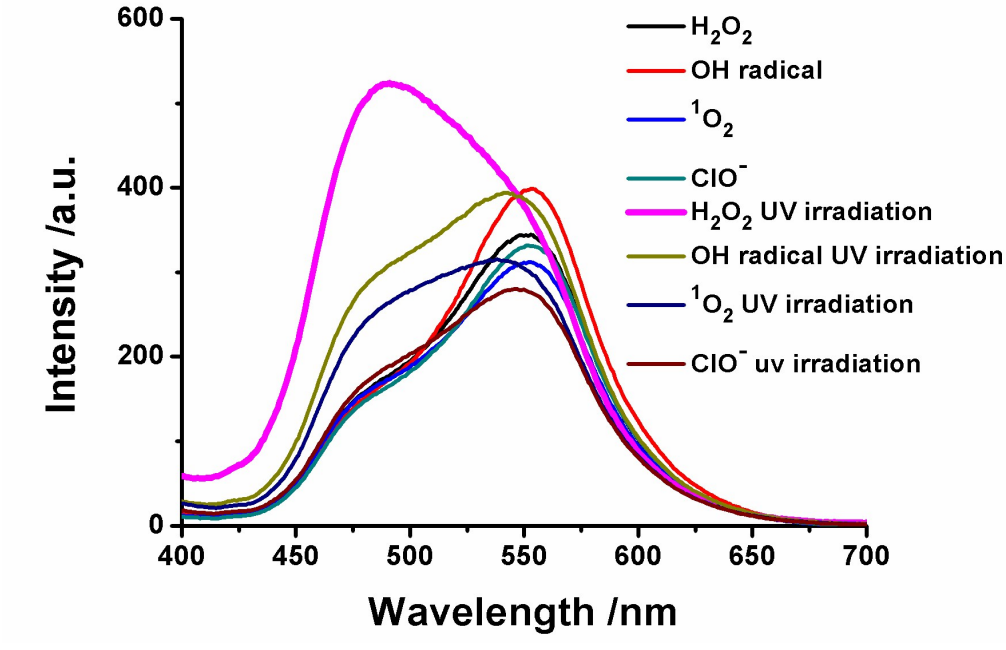

Figure S20. Fluorescent intensity of CSC (10^{-4} M) in H_2O/THF (9/1, v/v) with different ROS treatments.

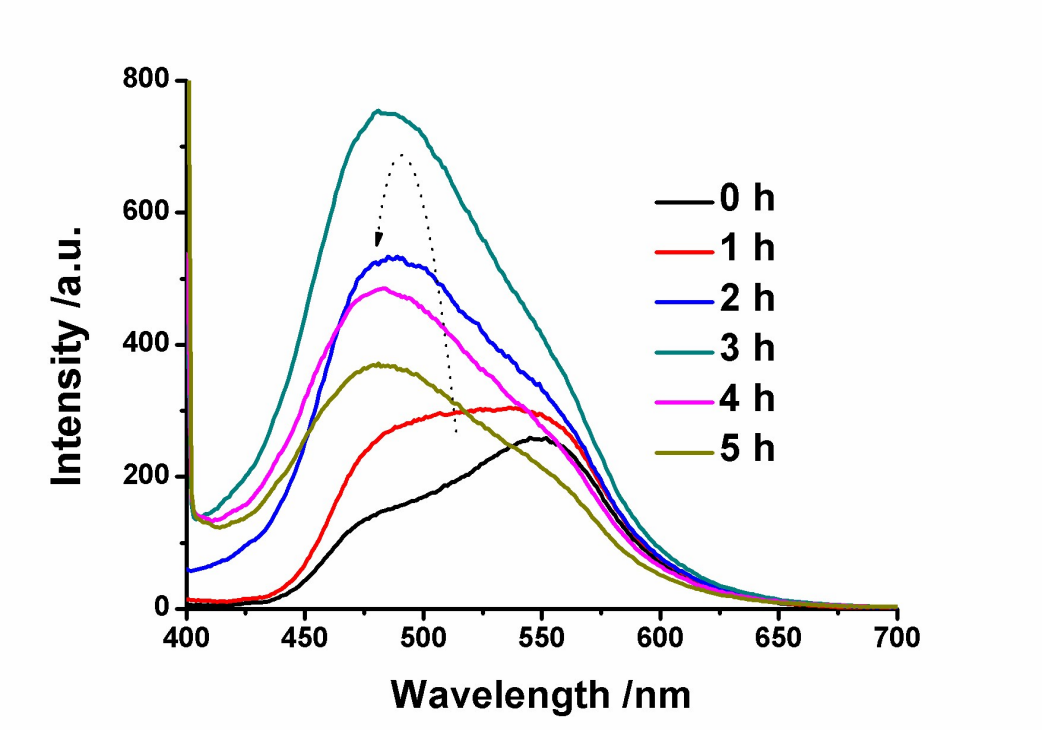

Figure S21 Time dependent emission spectra of CSC (10^{-4} M) in H_2O/THF (9/1, v/v) upon the addition of 1 molar equiv. H_2O_2 under UV light irradiation (254 nm).

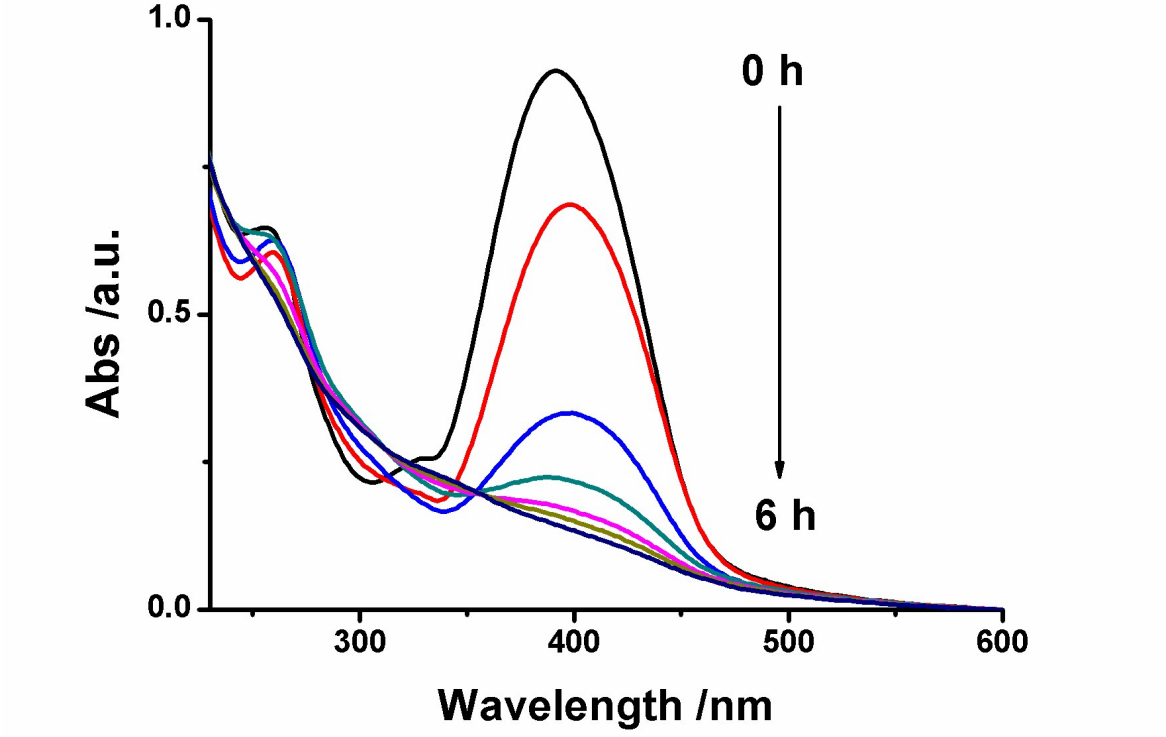

Figure S22. Time-dependent UV-visible spectra of CSC (10^{-4} M) in H_2O/THF (9/1, v/v) upon the addition of 1 molar equiv. H_2O_2 under UV light irradiation (254 nm).

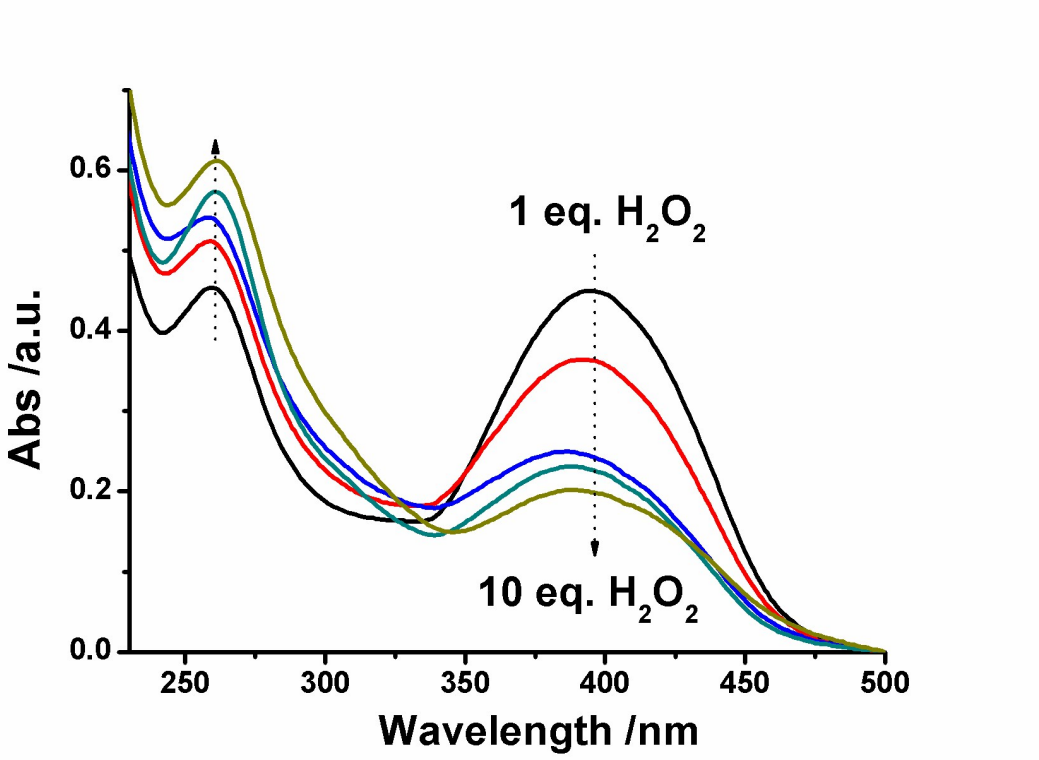

Figure S23. H_2O_2 concentration dependent absorption spectra of CSC (10^{-4} M) in H_2O/THF (9/1, v/v) under 1h UV light irradiation.

5. References

S1. L. Zhu, C. Y. Ang, X. Li, K. T. Nguyen, S. Y. Tan, H. Ågren and Y. Zhao, *Adv. Mater.*, 2012, **24**, 4020.

S2. (a) Y. Zhou and D. Yan, *J. Am. Chem. Soc.*, 2005, **127**, 10468; (b) W. Su, Y. Luo, Q. Yan, S. Wu, K. Han, Q. Zhang, Y. Gu and Y. Li, *Macromol. Rapid Commun.*, 2007, **28**, 1251; (c) *Adv. Mater.* 2007, **19**, 1752.

S3. (a) T. Sun, Q. Guo, C. Zhang, J. Hao, P. Xing, J. Su, S. Li, A. Hao and G. Liu, *Langmuir*, 2012, **28**, 8625; (b) A. Jesorka, M. Markstrom, M. Karlsson and O. Orwar, *J. Phys. Chem. B*, 2005, **109**, 14759.

S4. J. N. Israelachvili, Intermolecular and surface forces, Academic Press, New York, 1992.

S5. D. Wang, R. Dong, P. Long and J. Hao, *Soft Matter*, 2011, **7**, 10713.